On the chemical fate of propyl gallate as stabilizer in Lyocell spinning dopes

Melikhov, Ivan; Bacher, Markus; Hosoya, Takashi; Hettegger, Hubert; Potthast, Antje; Rosenau, Thomas

Published in:
Cellulose

DOI:
10.1007/s10570-023-05183-y

Published: 01/05/2023

Document Version
Final published version

Document License
CC BY

Cellulose (2023) 30:5373–5390
https://doi.org/10.1007/s10570-023-05183-y

ORIGINAL RESEARCH

On the chemical fate of propyl gallate as stabilizer in Lyocell spinning dopes

Ivan Melikhov · Markus Bacher · Takashi Hosoya · Hubert Hettegger · Antje Potthast · Thomas Rosenau

Received: 3 February 2023 / Accepted: 3 April 2023 / Published online: 15 April 2023

Abstract Propyl gallate (PG, gallic acid propyl ester, Tenox®) is a very frequently used stabilizer and antioxidant in food and material applications, also used on large scale in the Lyocell process to stabilize the cellulose spinning dopes. In the present study we have investigated the fate of PG under classical Lyocell conditions (cellulose dissolved in *N*-methylmorpholine-*N*-oxide monohydrate at temperatures above 80 °C) by means of multiple analytical techniques, including NMR, GPC, and MS-hyphenated chromatography. It is demonstrated that propyl gallate is quickly hydrolyzed to gallate or, as a side reaction, aminolyzed to gallic acid morpholide. The products of the antioxidative action of gallic acid and propyl gallate, namely ellagic acid and its bis(*ortho*-quinone), are very easily adsorbed to cellulosic surfaces and are chiefly responsible for the discoloration of Lyocell spinning dopes and the resulting fibers. However, gallic acid morpholide and its parent compound gallic amide, while both having good antioxidant activity similar to propyl gallate itself, do neither form ellagic acid nor the bis(*ortho*-quinone) and are thus significantly superior to the conventionally used propyl gallate with regard to chromophore generation and resulting brightness loss. Also gallate moieties in tannins can be converted into the amide or morpholide to be further used as Lyocell stabilizers, which might open the way both to new Lyocell stabilizers and to a niche utilization for tannins.

I. Melikhov · M. Bacher · H. Hettegger (✉) · A. Potthast · T. Rosenau (✉)
Department of Chemistry, Institute of Chemistry of Renewable Resources, University of Natural Resources and Life Sciences, Vienna (BOKU), Muthgasse 18, 1190 Vienna, Austria
e-mail: hubert.hettegger@boku.ac.at

T. Rosenau
e-mail: thomas.rosenau@boku.ac.at

T. Hosoya
Graduate School of Life and Environmental Sciences, Kyoto Prefectural University, Shimogamo-hangi-cho 11-5, Sakyo-ku, Kyoto-shi, Kyoto, Japan

T. Rosenau
Faculty of Science and Engineering, Laboratory of Natural Materials Technology, Åbo Akademi University, Porthansgatan 3, 20500 Åbo/Turku, Finland

Graphical abstract

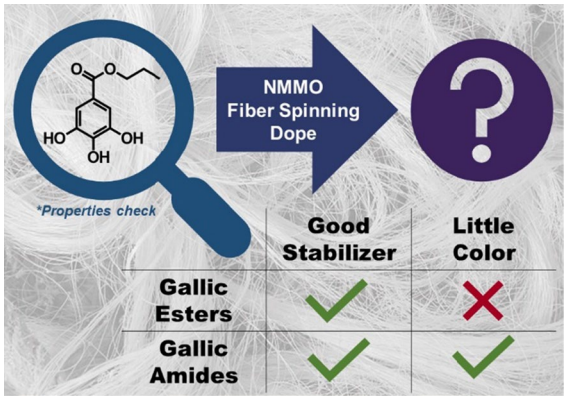

Keywords Antioxidant · Brightness · Cellulose · Cellulosic fibers · Chromophores · Fiber spinning · Lyocell · NMMO · Propyl gallate · Yellowing

Introduction

Propyl gallate (**1**, PG, Tenox®), the *n*-propyl ester of the common natural product gallic acid (3,4,5-trihydroxybenzoic acid, **2**), is a very frequently used stabilizer and antioxidant, which is compatible with aqueous systems, organic solutions as well as hydrophilic or hydrophobic polymers. Its good solubility properties, as well as its favorable toxicological characteristics, form the basis for its wide range of applications (Becker 2007; Akanbi and Barrow 2018; Decker et al. 2010; Zhang et al. 2006; Kahl 1984). Since the 1950s it has been used to prevent food from autoxidation during processing and storage (Walton et al. 1999; Adegoke et al. 1989; Oswell et al. 2018), in particular fats and oils, and has found similar uses in cosmetics, paints, adhesives (Kumar et al. 2021) and biofuels (Shameer and Nishath 2019; Yiin et al. 2014). As a food additive it is known as E310 in the EU. PG has been established to be innocuous, having no toxicological, mutagenic or carcinogenic effects (Hirose et al. 1993; Dolatabadi and Kashanian 2010; Kawanishi et al. 2005; Anderson et al. 1982) and even to offer some therapeutic potential in neurodegenerative diseases (Shalini et al. 2014; Ow and Stupans 2003). More recent studies, however, also suggest several negative effects (Wang et al. 2021), such as hormonal activities (Amadasi et al. 2009), pro-oxidative activity (Kobayashi et al. 2020) and allergenic potential (Holcomb et al. 2017; Gamboni et al. 2013).

As a classical phenolic antioxidant, PG acts as a trap of radicals and halts or minimizes autoxidative processes (Gregor et al. 2005). In this radical scavenger function it has often been used also in cellulose science, mostly to stabilize the polymer during processing against chain degradation and unwanted oxidation/autoxidation. It thus became the standard antioxidant used under "Lyocell conditions", i.e., cellulose solutions in *N*-methylmorpholine-*N*-oxide monohydrate (NMMO) at temperatures above approx. 80 °C, for the preparation of spinning dopes in the manufacture of cellulosic fibers (Firgo et al. 1995; Fink et al. 2001). In this process, PG had been originally introduced in an endeavor to chelate and thus neutralize transition metal ions, which had a detrimental effect on dope stability and cellulose integrity by inducing radical processes (Marini and Brauneis 1996). Later, it was established that the observed dope instabilities were largely a consequence of the formation of transient and highly reactive ionic intermediates, *N*-(methylene)morpholinium ions, which can degrade NMMO autocatalytically (Rosenau et al. 1999). Interestingly, PG showed a very high binding capacity also for those intermediates. This "double activity" against both transition metal ion-induced homolytic (radical) reactions and carbenium-iminium ion-induced heterolytic (ionic) degradation processes has rendered PG a quasi-ideal stabilizer for Lyocell spinning dopes, and the standard in particular for large, industrial-scale applications (Rosenau et al. 2002; Zhang et al. 2018). Early on, it has been noted that the stability benefits came at the expense of a strong discoloration of spinning dope and fibers (Rosenau et al. 2002, 2005a), which was, however, easily counteracted by mild alkaline washing and bleaching (Öztürk et al. 2009). Apart from minor amounts of cellulose-derived chromophores as a product of cellulose oxidation (Korntner et al. 2015; Ahn et al. 2019), the dark discoloration was mainly caused by byproducts of the stabilizer itself (Rosenau et al. 2002): its primary reaction product ellagic acid (**3**) forms a deeply colored bis(*ortho*-quinone) (**4**) when being further oxidized (see Fig. 1).

Over time, the pairing of PG with NMMO became a routine, so that this combination was also used in other larger-scale applications in biorefineries,

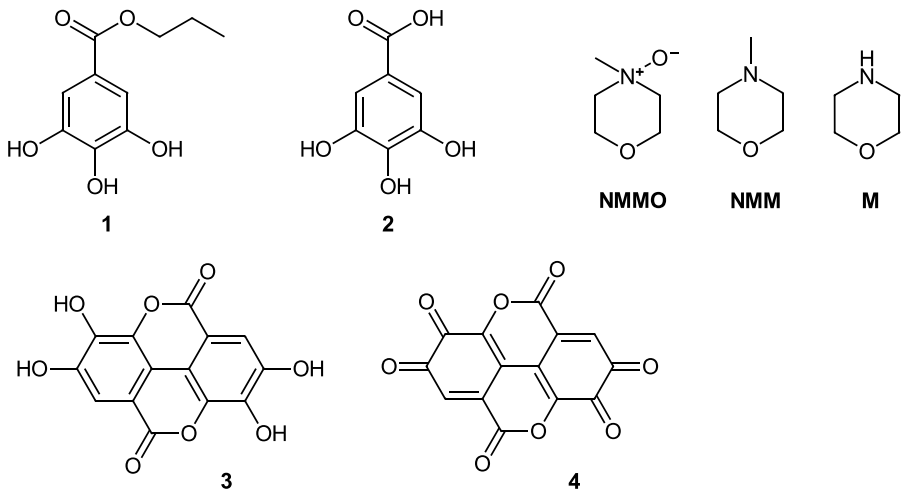

Fig. 1 Chemical structures of PG and its main reaction products as well as of *N*-methylmorpholine-*N*-oxide (NMMO) and its main degradation products *N*-methylmorpholine (NMM) and morpholine (M)

where the swelling, activation and pretreatment agent NMMO was usually accompanied by PG as a stabilizer, but also in small-scale applications of NMMO, such as chemical synthesis (Albini 1993; Coleman et al. 2000; Yokota et al. 2008) or material science (Erdman et al. 2016; Kulpinski et al. 2012; Skwierczyńska et al. 2019; Smiechowicz et al. 2018). Mostly concentrations of 0.5–2 wt% PG relative to the amine *N*-oxide are used. Especially in biorefinery settings, PG is often used regardless of the actual biorefining purpose, be it for biogas production (Aslanzadeh et al. 2014; Taherzadeh and Karimi 2008; Teghammar et al. 2012), enzymatic hydrolysis and saccharification (Khodaverdi et al. 2012; Kuo and Lee 2009; Liu et al. 2011), bioethanol production (Cai et al. 2016; Goshadrou et al. 2013; Poornejad et al. 2013; Shafiei et al. 2010), bio-pulping and biomass fractionation (Wikandari et al. 2016), and regardless of whether autoxidative processes actually occur and a stabilizer would be needed or not.

Apart from the identification of the main products of PG under conditions of Lyocell fiber production (cf. Figure 1), literature has been silent about the chemical fate of the stabilizer in all of these various application scenarios. The research concentrated on degradation reactions and byproduct formation of cellulose and NMMO, but the stabilizer has always been somewhat neglected: detailed side reactions, byproduct formation, consumption kinetics and the fate of the main degradation products are unknown. In our study about the chemical fate of propyl gallate, we came across the interesting fact that the minor degradation product gallic acid morpholide (**7**) was quite stable and showed much less subsequent chromophore formation than gallic acid or gallic esters. This behavior was extended to other gallic amides and elaborated further, so that gallic acid amides can be proposed as promising alternatives to propyl gallate, which is currently used exclusively in industrial-scale Lyocell fiber manufacture. Moreover, as we will show, gallic acid amides can be readily obtained from natural sources of gallates, such as tannins. With this account, we would like to contribute to a better understanding of the chemical fate of PG, taking the stabilization of Lyocell spinning dopes—its most important and prominent application—as an example. Based on this particular application case, we hoped to derive some general conclusions on the nature of PG reactions in the presence of NMMO, their kinetics and conversion products—not just under idealized lab settings, but also under real-world process conditions.

Materials and methods

General

All chemicals were commercially available and of the highest purity available. Thin layer chromatography (TLC) was performed on silica gel 60 plates (5 × 10 cm, 0.25 mm) with fluorescence detection under UV light at 254 nm. *N*-Methylmorpholine-*N*-oxide was recrystallized from dioxane, *N*-methylmorpholine-*N*-oxide monohydrate from acetone. [*R,R,R*]-α-Tocopherol was available from previous work (Rosenau et al. 2005b) and

N-methyl-tocopheramine was prepared by *N*-demethylation of the readily accessible respective dimethyl derivative (Rosenau et al. 2004). The cellulosic pulps used were a beech (*Fagus sylvatica*) sulfite pulp supplied by Lenzing AG, Austria, and a eucalypt (*Eucalyptus globulus*) Kraft pulp obtained from ENCE Group, Spain. The pulp parameters are summarized in Table 1.

Analysis and compound identification by nuclear magnetic resonance (NMR) spectroscopy

For NMR analysis, a Bruker Avance II 400 instrument (^{1}H resonance at 400.13 MHz, ^{13}C resonance at 100.62 MHz) with a 5 mm liquid N_2 cooled probe head (Prodigy) equipped with z-gradient with standard Bruker pulse programs was used. Data were collected with 32 k data points and apodized with a Gaussian window function (GB = 0.3) prior to Fourier transformation. A 2.5 s acquisition time and a 1 s relaxation delay were used. Bruker TopSpin 3.5 software was used for the acquisition and processing of the NMR data. Spectra were recorded in $CDCl_3$ in the case of isolated compounds (either from degradation mixtures or authentic samples for comparison), or in DMSO-d_6 for determination of the composition of the reaction mixtures. Chemical shifts, relative to TMS as an internal standard, are given in δ ppm values, coupling constants in Hz. ^{13}C peaks were assigned by means of APT, HSQC and HMBC spectra.

GC–MS analysis (liquid phase)

The sample (ca. 0.1 g) was dissolved in dichloromethane (ca. 2 mL). An aliquot (0.5 mL) was added to anhydrous pyridine (200 µL) containing 4-dimethylaminopyridine (DMAP, 1.5 mg/mL) and *N*,*O*-bis(trimethylsilyl)trifluoroacetamide (BSTFA, 200 µL) containing 10% trimethylchlorosilane (TMCS). The mixture was heated for 2 h at 70 °C, cooled to room temperature (RT), diluted to 1.00 mL with dichloromethane and analyzed. Instrument: Agilent 7890A gas chromatograph with an Agilent 5975C triple axis mass selective detector (MSD); column: DB5-ms (30 m × 0.25 mm i.d., 0.25 µm film thickness; J&W Scientific, Folsom, CA, USA); MMI multi-mode inlet: splitless injection (0.2 µL), constant column flow, carrier gas: helium (0.9 mL/min), purge flow: 15.0 mL/min (0.75 min); injector: constant T = 260 °C, temperature profile: 50 °C (2 min), then 5 °C/min to 280 °C (20 min). MS detection: EI mode, 70 eV ionization energy, 1.13×10^{-7} Pa, ion source temperature: 230 °C, quadrupole: 150 °C, transfer line: 280 °C, data acquisition: scan from 45

Table 1 Characteristics of the cellulosic pulps used

	Beech sulfite pulp	Eucalyptus Kraft pulp
Brightness (%ISO)	88.5	86.0
Kappa number	0.79	0.60
Intrinsic viscosity (mL/g)[1]	546	843
R18 (%)	93	92
Monosaccharide composition (wt%)[2]	Glucose 94.07 ± 0.08[3]	Glucose 77.55 ± 0.12
	Xylose 3.38 ± 0.01	Xylose 18.45 ± 0.06
	Mannose 0.77 ± 0.003	Mannose 0.11 ± 0.004
	Arabinose 0.00	Arabinose 0.03 ± 0.002
	Galactose 0.01 ± 0.001	Galactose 0.31 ± 0.001
	Rhamnose 0.00	Rhamnose 0.00
Crystallinity index[4]	0.56	0.48
Mw (kg mol^{-1})[5]	280	460

[1]Determined as cuen viscosity (in cupri-ethylenediamine) according to Ahn et al. (2019)

[2]Determined by total acid hydrolysis and subsequent analysis of the monosaccharides with anion-exchange chromatography

[3]Standard deviation as means from three independent measurements

[4]Determined by solid-state ^{13}C NMR according to Zuckerstätter et al. (2013) and Jusner et al. (2022)

[5]Determined by GPC according to Potthast et al. (2015)

to 950 m/z, autosampler: CTC-PALxt, Chronos software v.3.5 (Axel Semrau, Spockhövel, Germany). The NIST/Wiley 2008 database was used for compound identification.

Headspace GC–MS analysis (gas phase)

GC–MS analysis was carried out on an Agilent 6890 gas chromatograph with an Agilent 5975C mass selective detector (MSD). Column: VF-WAXms (30 m × 0.25 mm i.d., 0.25 µm film thickness; J&W Scientific, Folsom, CA, USA). MMI multimode inlet: splitless injection, constant column flow: 0.9 mL/min, carrier gas: helium, purge flow: 15.0 mL/min (0.75 min); injector: constant at 250 °C, temperature profile: 40 °C (2 min), then 8 °C/min to 250 °C (6 min); MS detection: EI mode, 70 eV ionization energy, 1.13×10^{-7} Pa, ion source temperature: 230 °C, quadrupole: 150 °C, transfer line: 280 °C; data acquisition: scan from 45 to 500 m/z; injection: 3 mL headspace, Agilent 7694 headspace sampler, 3 min equilibration at 50 °C, vial pressurization time: 0.2 min, loop fill time: 0.18 min, loop equilibration time: 0.05 min, injection time: 1 min. The NIST/Wiley 2008 database was used to support compound identification.

Degradation of Lyocell dopes and NMMO/cosolvent mixtures by cellulosic pulps

A computer-controlled IKA C-6000 bomb calorimeter with efficient stirring and efficient heating (50 °C/min) was used to prepare solutions of cellulosic pulps in NMMO, to follow degradation reactions in the spinning dopes and to test stabilizer efficiencies. Stabilizers (0.1 mol% rel. to NMMO) were added to aqueous NMMO at 50 °C or to a melt of *N*-methylmorpholine-*N*-oxide monohydrate at 80 °C. Cellulosic pulp (10 wt%) was added under efficient stirring to produce suspensions (aqueous NMMO at 50 °C) or solutions (NMMO at 80 °C). The vessel was closed immediately and time and pressure were recorded. The time to the onset of the spontaneous degradation ("t_{onset}"), seen in a sudden increase in temperature and pressure, was taken as a measure of the (in)stability of the mixture. Temperature, stabilizer and reaction parameters were subject to variations (see main text).

In some cases, the gas phase was withdrawn through the sample valve and analyzed by headspace GC–MS. For NMR analysis of the main NMMO degradation products, a 300 µL aliquot of the liquid phase was mixed with 300 µL of DMSO-d6 and analyzed by ^{1}H NMR.

For studies of the stabilizer chemistry, the liquid phase was poured into a saturated aqueous NaCl solution (100 mL, pH = 4 set with conc. HCl), stirred vigorously for 1 min and extracted with dichloromethane (3 × 20 mL). The organic extracts were combined. The pH of the aqueous phase was adjusted to 10 (2 M NaOH) and extracted again with dichloromethane (3 × 20 mL). The aqueous phase was discarded and all organic extracts (of both the acidic and alkaline aqueous phase) were combined, washed with saturated brine (20 mL) and dried over anhydrous $MgSO_4$. Evaporation of the solvent in vacuo was performed at RT in order not to lose highly volatile components. An aliquot of the residue was dissolved in $CDCl_3$ for NMR and GC–MS analysis. The bulk of the residue was dissolved in chloroform, subjected to column chromatography on silica gel with an ethyl acetate/toluene (v/v = 4:1) eluant. The isolated components were analyzed by NMR and GC–MS analyses (see above). The identity of the reported components was in all cases confirmed additionally by comparison with authentic samples, which were either commercially available or independently synthesized.

Synthesis of gallic acid amide and derivatives

The synthesis of pure gallic acid morpholide (**7**) was carried out in four steps according to Scheme 3. Gallic acid (**2**, 1.24 g, 7.3 mmol) was dissolved in dry DMF (35 mL), *tert*-butyldimethylsilyl chloride (TBS-Cl, 6.54 g, 43 mmol, 6 eq.), and imidazole (4.98 g, 73 mmol, 10 eq.) were added and the reaction mixture was stirred at RT for 24 h. The crude product was extracted with diethyl ether, the combined organic phases were washed with water and saturated brine, dried over anhydrous $MgSO_4$, filtered, and evaporated under reduced pressure yielding the tetrasilyl intermediate as a yellow oil (5.35 g of crude product). The protection method followed the protocol of Tan et al. (2019) with minor modifications.

Selective deprotection of the silyl ester was performed according to Morton and Thompson (1978) with modifications. The crude silylated gallic acid (5.35 g) in THF and MeOH (124 mL, 1:3 v/v) was added to a solution of K_2CO_3 (3.1 g, 22 mmol, 3 eq.)

in water (31 mL). After stirring for 2 h at RT, the reaction solution was concentrated on a rotary evaporator to about 25% of the starting volume, diluted with saturated brine (93 mL), and cooled to 0 °C in an ice/water bath. The pH was adjusted to 4–5 with a 2 M sodium hydrogensulfate solution, followed by extraction of the mixture with diethyl ether. The combined organic phases were washed with water and saturated brine, dried over anhydrous $MgSO_4$, filtered, and evaporated under reduced pressure to yield crude 3,4,5-tris(*tert*-butyldimethylsilyloxy)benzoic acid as a pale-yellow solid (5.85 g, $R_f = 0.60$, silica, $CHCl_3$/MeOH, v/v = 12:1).

The crude product (5.85 g) was dissolved in dichloromethane (100 mL) and cooled to 0 °C. DCC (3.5 g, 17 mmol), DMAP (200 mg, 1.6 mmol), and morpholine (4.0 mL, 46 mmol) were successively added to the solution. The reaction mixture was allowed to reach RT, stirred overnight, filtered and concentrated under reduced pressure. The residue (7.75 g) was purified by flash column chromatography (*n*-hexane/EtOAc, v/v = 4:1) to afford the protected amide, 3,4,5-tris(*tert*-butyldimethylsilyloxy)benzomorpholide, as a white solid (2.08 g, 3.57 mmol, 49% relative to gallic acid **2**). The amide coupling procedure was based on Thysiadis et al. (2018) with modifications.

Water (16 mL) and TBAF trihydrate (5.2 g, 16.5 mmol, 2 eq.) were added to the product from the previous step (1.62 g, 2.78 mmol) dissolved in THF (100 mL). The reaction mixture was stirred at RT overnight, resulting in a change of the color of the solution from dark green to orange. The mixture was extracted several times with dichloromethane and the combined organic extracts were dried over anhydrous $MgSO_4$, filtered, and evaporated. The residue was purified twice by flash column chromatography (eluent: $CHCl_3$/MeOH, v/v = 7:1) to afford pure gallic acid morpholide **7** as a pale-yellow solid ($C_{11}H_{13}NO_5$, 239.22 g mol^{-1}, 268 mg, 1.1 mmol, 40% relative to gallic acid **2**).

The synthesis of gallamide (**8**) was performed in a facile one-pot procedure (Scheme 3) which afforded the product at a purity of > 99% so that chromatographic purification appeared unnecessary. An aliquot was purified by flash column chromatography (eluent: $CHCl_3$/MeOH, v/v = 7:1) for analytical characterization. Gallic acid propyl ester (propyl gallate, **1**, 2.12 g, 10 mmol) was dissolved in dry toluene (50 mL) and ammonium formate (6.31 g, 10 eq.) was added during stirring. The mixture was refluxed for 1 h, cooled to RT and filtered. The solvent was removed in vacuo and the residue was recrystallized from dioxane to afford gallamide (**8**) as a pale-yellow powder ($C_7H_7NO_4$, 169.13 g mol^{-1}, 1.48 g, 88%).

The synthesis procedure for the conversion of gallotannins into the corresponding tannamide derivative (**9**) will be described elsewhere along with detailed analytical data.

Results and discussion

Analytical aspects

Table 2 summarizes the ^1H and ^{13}C NMR resonances of compounds **1**–**4** (Fig. 1), recorded in DMSO-d_6 as the solvent. Data available in the literature are inconsistent and hard to compare as they were recorded in different solvents or mixtures, at different temperatures and different concentrations. The data in Table 2 can be used as reference in PG-related work because the compounds were measured under identical and precisely set conditions. It is evident that ^1H NMR does not provide a good basis for the discrimination of the compounds, with only one proton at the aromatic core. Also the ^{13}C shift differences between corresponding atoms in the derivatives were rather small and neither typical nor meaningful with regard to compound distinction. While NMR is suitable to identify the neat compounds or to establish their presence in mixtures of sufficiently high concentrations, alternative methods are needed to detect the compounds in complex mixtures or at small concentrations.

For PG analysis, the literature suggests electrochemical detection (Chýlková et al. 2017) and quantification by liquid chromatography (Gómez-Hens and Godoy-Navajas 2015). We resorted to high-performance thin layer chromatography (HP-TLC), a technique which we have been exploiting for the separation of complex multicomponent mixtures and analytes with strong matrix interference which would prohibit the use of conventional HPLC due to column clogging or damage (Oberlerchner et al. 2018; Böhmdorfer et al. 2018; Syed Jaafar et al. 2013). Similar concerns with regard to HPLC were obviously also justified in the case of Lyocell spinning dopes, but

Table 2 ^{1}H and ^{13}C NMR resonances of PG (**1**) and its derivatives (**2 – 4**), analyzed as 20 mM solution in DMSO-d_6 at RT

	Propyl gallate (**1**)	Gallic acid (**2**)	Ellagic acid (**3**)	Ellago-quinone (**4**)[a]
C-1	119.7	120.6	112.5	115.8
C-2/H-2	108.6/6.95 (s, 2H)	108.9/6.91 (s)	107.6	118.6
C-3	146.1	145.6	136.5	144.8
C-4	138.5	138.2	139.8	177.4
C-5	146.1	145.6	148.2	180.2
C-6/H-6	108.6/6.95 (s, 2H)	108.9/6.91 (s)	110.3/7.44 (s)	114.9/8.06 (s)
COOR	166.0	167.6	159.3	156.0
Propyl	10.5/0.93 (t, 3H), 21.9/1.65 (qt, 2H), 65.6/4.10 (t, 2H)	–	–	–
OH	9.15 (OH-3/4/5)	8.83 (OH-4), 9.19 (OH-3/5), 12.23 (COOH)	8.92 (OH-4/5)	–

[a]2,3,5,7,8,10-Hexahydrochromeno[5,4,3-*cde*]chromene-2,3,5,7,8,10-hexaone

fortunately HP-TLC allowed a very easy and at the same time robust and accurate separation and detection of the target compounds.

The usual concentration of PG in Lyocell spinning dopes is 2 wt% relative to the dissolved cellulosic pulp, which usually has a concentration of about 10 wt%. This results in a 0.2 wt% PG starting concentration in the spinning dope, which was also used in our experiments.

As samples we used PG-stabilized Lyocell spinning dopes—at different stages of processing and by-product formation (see below)—which were diluted with distilled water (v/v = 1:4), and extracted with the same volume of a ternary solvent mixture (*n*-hexane/ethyl acetate/glacial acetic acid, v/v/v = 6:4:1), optimized based on the literature (Komaitis 1991). Upon mixing and extraction, the acetic acid remains in the aqueous phase, where it ensures an acidic medium in which phenolic hydroxy groups and the carboxy group of gallic acid are present in the protonated form. After two extractions of the aqueous medium with the same amount of organic phase, no remaining gallic or ellagic acid derivatives were detectable in the aqueous phase by UV/Vis spectroscopy, so the extraction was assumed to be quantitative. The same ternary solvent was used as the HP-TLC eluant as well. Besides PG, gallic acid and ellagic acid, also other gallic esters and gallic acid amides (data not shown) were reliably separated and detected with this system. The presence of acetic acid in the eluant was imperative to minimize the drag trace typical of gallic acid derivatives and polyhydroxy-aromatics in general. In automated HP-TLC mode (sampling, development and scanning/quantification) of solution with 0.1 mg mL^{-1} dissolved organics, PG was quantifiable when present between 0.25 and 100% of the dissolved dry matter, and detectable—although not quantifiable—down to 0.05%. This seemed to be fully sufficient as an analytical approach, even for kinetic studies.

The chemical fate of PG under Lyocell conditions

The chemical integrity and the reactions of PG depend on the medium and the conditions of its application. Two general sets of conditions are of practical relevance in Lyocell fiber production: first, aqueous NMMO of about 50 wt% water which is used to swell the cellulosic pulp at temperatures between RT and about 50 °C; and second, the solution of cellulose in NMMO monohydrate (or a binary NMMO/water mixture of roughly equimolar composition) at temperatures between 80 and 100 °C. Depending on at which time in the process the PG is added to the NMMO/cellulose mixture, the stabilizer is exposed to either condition or both conditions. The two sets of conditions, 50% aqueous NMMO at 50 °C and NMMO monohydrate at 80 °C, were also used in our experiments.

When preparing the monohydrate and the aqueous solution from freshly recrystallized NMMO, which was free of degradation products, PG (0.2 wt%, see above) showed high stability under both conditions. In 50% aq. NMMO at 50 °C, degradation of PG was

less than 3% after 2 h, in NMMO monohydrate at 80 °C less than 8%, the small amount of consumed PG being hydrolyzed to gallic acid (**2**) (Fig. 2).

However, under real-world industrial conditions of cellulose fiber manufacture, NMMO is never pure, but contains *N*-methylmorpholine (NMM) and morpholine (M) as its two typical, almost ubiquitous degradation products. The molar ratio of NMM and M ranges usually between 3:1 and 5:1 (Marini and Brauneis 1996; Zhang et al. 2018). The concentration of the degradation products varies from less than 0.1 wt% in freshly purified NMMO and 3.5 wt% in NMMO shortly before the recycling/purification step (the byproduct percentages refer to the NMMO used). In our experiments we added 2 wt% of a 4:1 mixture of NMM and M to the NMMO in order to simulate the usual industrial conditions as realistically as possible.

The presence of these byproducts changed the stability of PG drastically. In 50% aq. NMMO at 50 °C—now containing 2 wt% of a 4:1 mixture of NMM and M—PG was completely consumed after 2 h (Fig. 2). A rough kinetics recorded over the time of 2 h showed that the major part of PG (94%) was consumed already during the first 15 min after addition, being converted into gallic acid (**2**), besides traces (less than 2%) of ellagic acid (**3**). The presence of cellulosic pulp had no obvious influence on PG consumption.

The consumption of PG meant a simultaneous release of 1-propanol which was detected after 20 min in the gas phase above the Lyocell dope by headspace-GC-MS. The confirmation that this alcohol indeed originated from the PG and not from another degradation process was provided by using butyl gallate instead of PG in one experiment. The gas phase contained 1-butanol in this case, which was detected analogously by headspace-GC-MS. Quantification was not performed in either case.

The consumption of PG in 50% aqueous NMMO containing NMM/M impurities is simply due to a base-catalyzed hydrolytic process. The interesting fact was that PG was almost completely consumed already after 15–20 min. This raises the question of how reasonable (and economical) it is to use PG as a stabilizer instead of simply using gallic acid, since after a short time only gallic acid would be present anyway—and no longer PG. A 50 wt% aqueous solution of pure NMMO (molar ratio NMMO/water = 1:6.5) has a neutral pH value. However, the presence of the amine degradation products drastically increases the pH since both NMM and M are organic bases and their aqueous solutions show a relatively strong alkaline behavior. A 2 wt% NMM/M mixture (4:1) has a pH of 11.2 in water at 50 °C, and 11.4 in aqueous NMMO (50%) at RT. The pK_B values of M and NMM are 5.64 and 6.62. The alkalinity of the mixture was evidently sufficient to effect fast and quite complete hydrolysis of PG. At the prevailing pH, the resulting gallic acid is primarily present as gallate anion, balancing the morpholinium and *N*-methylmorpholinium cations. Considering that—due to the small amount of PG used (usually 0.2 wt% relative to NMMO)—the alkaline NMMO degradation products are present in roughly stoichiometric amounts, it becomes clear that—from the perspective

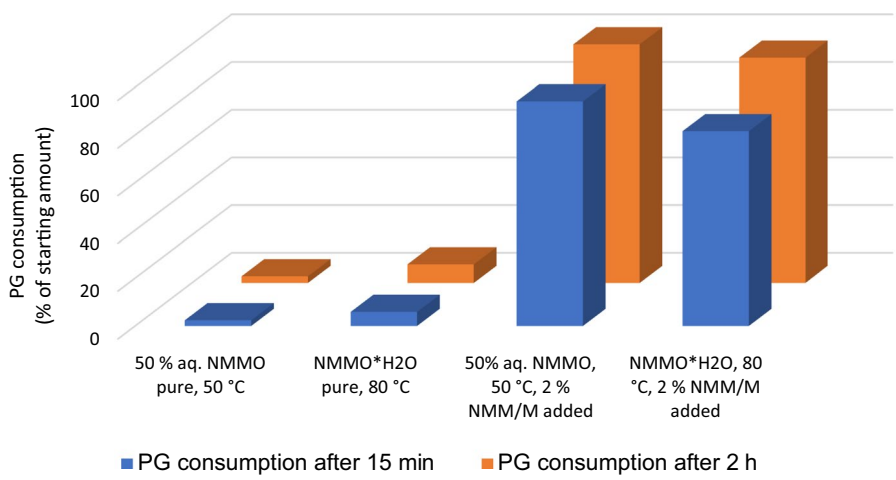

Fig. 2 Consumption of PG after 15 min and 2 h under different conditions: **a** 50 wt% aq. NMMO at 50 °C, either pure or containing 2 wt% (rel. to NMMO) of a 4:1 mixture of NMM and M; **b** NMMO monohydrate at 80 °C, either pure or containing 2 wt% (rel. to NMMO) of a 4:1 mixture of NMM and M

of PG—the hydrolysis is a dominant process rather than a minor side reaction (see Fig. 3).

Figure 3 displays the dependence of the hydrolysis rate of PG on the reaction conditions, namely temperature, base concentration (4:1 NMM/M mixture), and reaction medium (water, 50% aqueous NMMO and 50% aqueous NMMO with 10 wt% suspended cellulosic pulp). The consumption of PG was measured 15 min after PG addition. At 50 °C, the hydrolysis was generally faster than at RT, the difference being rather constant. Only at very low concentrations of NMM/M (0.01% and 0.1%) the presence of pulp had a significant influence, but at NMM/M concentrations of 1% and above this effect became negligible. Cellulosic pulps have only a small buffer/ion exchange capacity (which is not to be confused with the chelating capability). Minor amounts of NMM/M can be "neutralized" by the low content of carboxy groups in cellulose and mainly in residual xylans, but this effect is rather small and fails to compensate for higher NMM/M concentrations. The slightly higher PG stability in the presence of pulp 2 (Eucalyptus Kraft pulp, see Fig. 3 and Materials and methods section), as compared to pulp 1 (beech sulfite pulp), might indicate a better deactivation of the base impurities NMM and M by the higher amount of carboxy functions in the former. In general, the NMM/M concentration was the dominant factor influencing PG stability. Down to an NMM/M concentration of 0.1 wt%, PG hydrolysis remained dominant with more than 50% of the compound having reacted after 15 min.

It should be emphasized that the hydrolysis of PG does not mean a loss of the antioxidative, complexing and carbenium-iminium ion-scavenging properties, for which the stabilizer is being used. These properties are due to the phenolic OH of the gallate moiety and are largely independent of the carboxy group being esterified or not. Subsequent antioxidant chemistry proceeds via the 3,4,5,3′,4′,5′-hexahydroxydiphenic acid intermediate, which is either present as the free acid (**5**) in the case of PG hydrolysis or as the bis(*n*-propyl ester) (**6**) in the case of PG. Both intermediates readily form ellagic acid (**3**)—and later on the ellago-quinone (**4**)—no matter if the carboxy moiety is free or still esterified (see Scheme 1).

In molten NMMO monohydrate (80 °C), consumption of PG after 15 min and 2 h was 72% and 85%, respectively, compared to 94% and 100%, respectively, in 50% aqueous NMMO at 50 °C (see Fig. 2). At a first glance, this slower reaction under the more drastic conditions seems surprising. However, one should remember that the water in NMMO monohydrate is tightly bound into ribbon-like hydrogen bond networks and is not free to (re)act like bulk water (Rosenau et al. 2001). The reactivity of NMM and M in NMMO monohydrate will thus be different from aqueous NMMO, and their alkalinity cannot unfold in the absence of bulk water. For the same reason, measuring a pH value in NMMO monohydrate is meaningless. This view was supported by the fact that not only the consumption of PG was slightly slower, but also a different product mixture was obtained, proving the

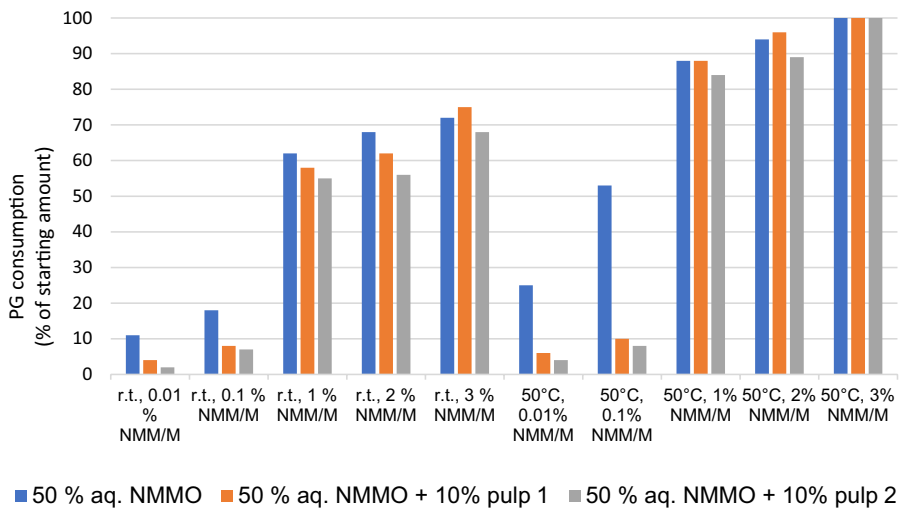

Fig. 3 Dependence of PG consumption, measured 15 min after PG addition, on different temperatures (RT, 50 °C), different concentrations of a 4:1 NMM/M mixture, and the presence of suspended cellulosic pulps (10 wt%, see Materials and methods)

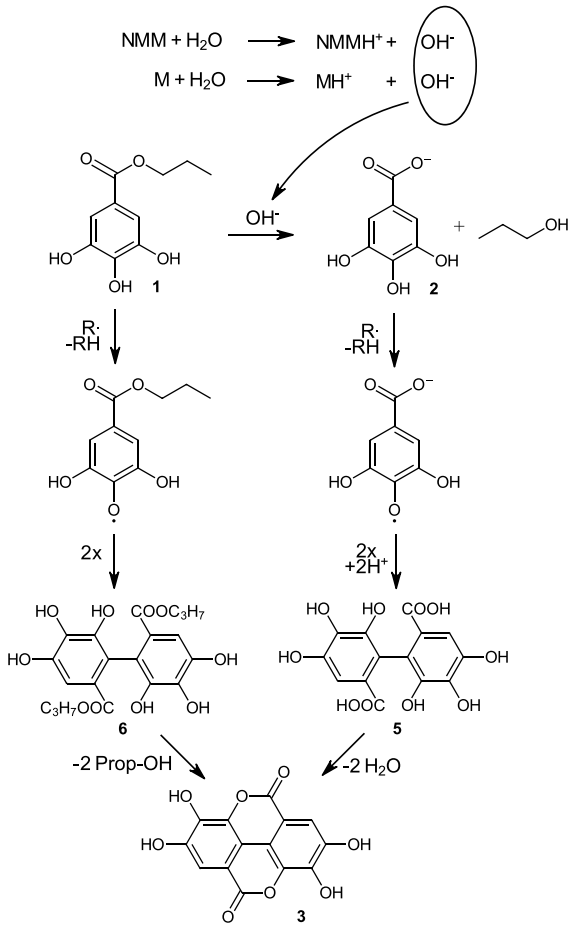

Scheme 1 PG hydrolysis in aqueous NMMO by the NMMO degradation products *N*-methylmorpholine (NMM) and morpholine (M) and subsequent reactions

occurrence of reactions other than the simple alkaline hydrolysis of the ester.

In NMM/M-doped NMMO monohydrate, two products were formed from PG in a roughly equimolar ratio: the hydrolysis product gallic acid (more correctly, the gallate anion) and another product of which the NMR spectrum indicated the presence of both a gallate and a morpholine moiety. Temperature-dependent NMR measurements showed the morpholine´s two *N*-methylene groups to be magnetically inequivalent at RT, but to coalesce at about 50 °C. This pointed to the participation of morpholine´s nitrogen in an amide bond and rendered it likely that the product was gallic acid morpholide (morpholinyl gallamide, **7**).

In NMM/M-doped NMMO monohydrate, PG was thus not only hydrolyzed as in aqueous NMMO, but also partly converted into the corresponding morpholide derivative. Apparently, the reaction of PG with morpholine became more dominant with decreasing water content and increasing temperature. It should be noted that—from the viewpoint of the reaction mechanism—the formation of gallic acid morpholide (**7**) is an aminolysis of PG as a gallic acid ester, but not a direct amidation reaction between gallic acid and morpholine (Scheme 2). If gallic acid was used instead of PG under otherwise identical experimental conditions, no gallic acid morpholide whatsoever was formed (but morpholinium salts of gallic acid), proving PG aminolysis by morpholine as the formation mechanism.

Scheme 2 PG aminolysis in NMMO monohydrate by the NMMO-degradation product morpholine (M) to gallic acid morpholide (**7**) and resonance structures of the morpholide

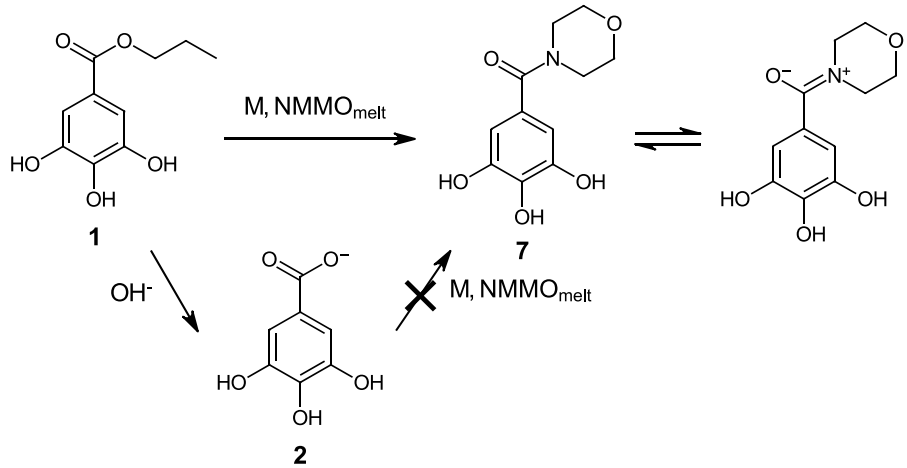

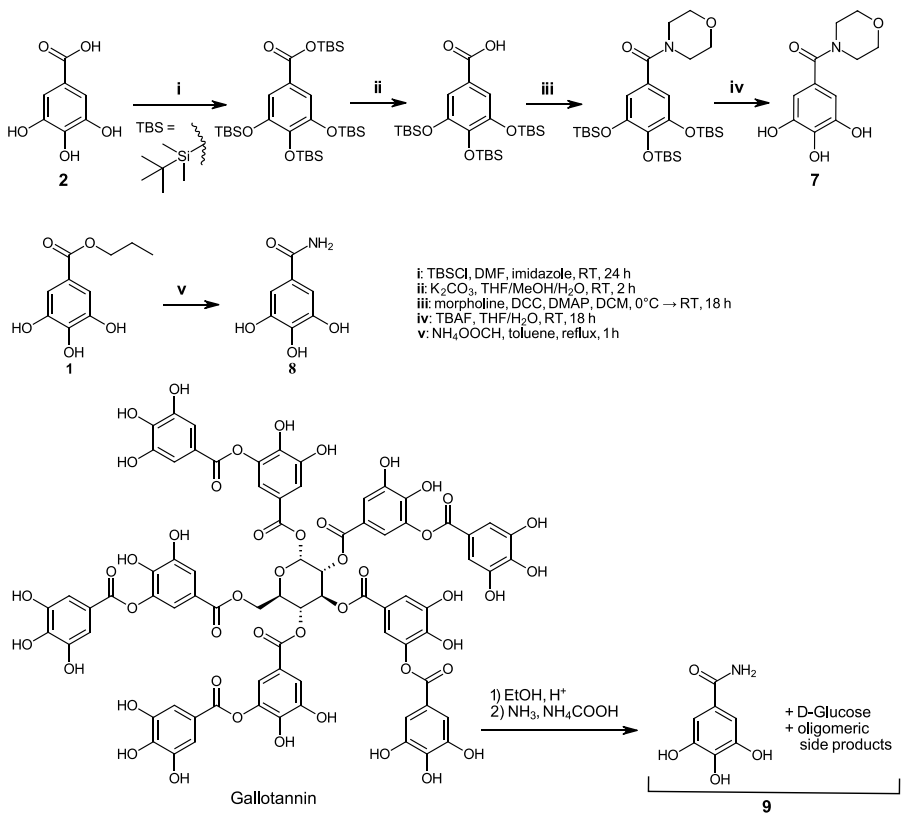

Scheme 3 Chemical syntheses of authentic samples of gallic acid morpholide (**7**) and gallamide (**8**) as well as conversion of a gallotannin to "tannamide" (**9**), a mixture containing a significant fraction of gallamide moieties. The gallotannin structure given shows the principal structural elements of the depside-type compound family

Synthesis of amide derivatives of gallic acid

To verify the structure of compound **7**, we attempted the independent synthesis of the compound to prove the structure by comparison of the isolated with a synthesized authentic sample. However, this seemingly straightforward synthesis appeared to be astonishingly tricky. Note that direct amidation and ester aminolysis is usually very sluggish for secondary amines (morpholine) and that, in addition, amidations involving gallic acid or hydroxy-protected galloyl chloride are always accompanied by prominent self-esterification (depside formation) and by strong discoloration and ellagic acid formation if not carried out under strictest exclusion of oxygen. We finally resorted to a protecting group approach, which involved more steps but was able to provide the target compound **7** in pure form via well-characterized intermediates (Scheme 3). Analytical evaluation of synthesized and isolated variants of **7** confirmed their identity (see Table 3).

For reasons of comparison, we also synthesized gallamide (**8**), the parent compound of gallic acid morpholide (**7**). In this case, the direct reaction of PG with ammonia proceeded neatly, very different from the reaction with morpholine, so that the detour via protected derivatives was unnecessary (Scheme 3). Ammonia was introduced as ammonium formate which, on the one hand, provided the necessary NH_3 for ester aminolysis and, on the other hand, generated a mildly reducing medium that prevented oxidative side reactions and discoloration through the gallate moiety.

Since gallic acid derivatives are still relatively costly, we used tannic acid (gallotannin), with its naturally high content of gallic acid moieties, as a bulk substitute which is potentially economically more attractive. Tannins are secondary plant compounds that are generally considered non-toxic and even have a health-promoting effect as neutraceuticals. They are bulk products in the food and leather industries and in some variants of biorefineries. Tannic acid (gallic acid content 82%) was converted into the amides by reaction with concentrated aqueous ammonia (with or without previous transesterification with ethanol). The gallamide content in the reaction product was

Table 3 ^{1}H and ^{13}C NMR resonances of gallamide (**7** – **9**), measured as 20 mM solutions in DMSO-d_6 at RT

	Gallic acid morpholide (**7**)[a]	Gallamide (**8**)	Tannamide (**9**)
C-1	125.2	124.7	112.5
C-2/H-2	106.6/6.31 (s)	107.2/6.81 (s)	106.9–107.6/6.52–6.84
C-3	145.7	145.6	145.3–145.6
C-4	134.8	136.4	135.8–137.1
C-5	145.7	145.4	145.3–145.6
C-6/H-6	106.6/6.31 (s)	107.2/6.81 (s)	106.9–107.6/7.44 (s)
CO–NR_2	169.6	168.4	159.3
	morpholine: N–CH_2: 44.6 and 57.5/3.45 (m, 4H), (O–CH_2): 65.7 and 66.3/3.55 (m, 4H); ^{15}N NMR: n.d	NH_2: 6.80 (s, 1H), 7.60 (s, 1H); ^{15}N NMR: − 280 ppm	NH_2: 6.20–8.40 (br); ^{15}N NMR: − 287 to − 275 ppm

[a]measured at 353 K (80 °C)

estimated to be 87% according to elemental analysis, indicating a near-quantitative amidation of the contained gallates. The synthesis and analytical aspects of the gallotannin derivatives will be reported in detail elsewhere.

Table 3 summarizes the NMR data (^{1}H and ^{13}C chemical shifts) of the amide derivatives **7** – **9** (Scheme 3). Due to the hindered rotation of the amide bond, the two *N*–CH_2 groups in the morpholino moiety of **7** become magnetically inequivalent. Tannamide (**9**) is a pale-yellow powder, a mixture of monomeric gallamide (**8**), along with oligophenolic and polyphenolic gallamide moieties and with D-glucose that was released upon the transesterification/amidation sequence (Scheme 3).

Comparison of gallic acid and its ester and amide derivatives in Lyocell dopes with regard to stabilizing effect and chromophore generation

Since gallic acid and its ester PG were similarly effective as Lyocell stabilizer, it was interesting to see whether also gallic acid amides would retain the stabilizing effect or whether the part of PG which is converted to the amides under Lyocell conditions would become more or less ineffective in terms of dope stabilization. Traces of transition metal ions (25 ppm of Fe(II) sulfate) were used to induce homolytic and heterolytic degradation of NMMO, and a slightly elevated temperature of 100 °C was applied, along with 10 wt% of dissolved pulp. The t_{onset} times, i.e., the periods until the irreversible, highly exothermic degradation of the dope started, were recorded as a measure of dope stability/stabilizer efficiency.

While the non-stabilized dope had a t_{onset} of only about 55 min, some common natural antioxidants, such as α-tocopherol and α-tocopheramine, and synthetic antioxidants, such as butylated hydroxyanisole (BHA) and butylated hydroxytoluene (BHT), exerted a certain stabilizing effect (t_{onset} between 90 and 115 min). This effect, however, was small against the very effective stabilization of the dope by PG, gallic acid and the gallic amide derivatives, which gave very large t_{onset} times, generally above 400 min, see Fig. 4. There were no significant differences between the three amide derivatives (**7**, **8** and **9**): their t_{onset} times were very similar (Fig. 4). All stabilizers were used at the same molar concentrations of 0.2 mol% rel. to NMMO monohydrate (see above). While α-tocopherol, α-tocopheramine, BHA and BHT, as radical chain-breaking antioxidants, act against homolytic (radical) side reactions, they are not effective against carbenium-iminium ions, which induce the autocatalytic degradation of NMMO (Rosenau et al. 1999). The gallate derivatives, by contrast, scavenge these intermediates by electrophilic substitution at their free aromatic ring positions (Rosenau et al. 2002; Zhang et al. 2018). Differences between the different stabilizers in terms of cellulose integrity and oxidative damage of the dissolved pulp are the topic of a follow-up report.

An interesting observation was made during the experiments with gallic amide derivatives as Lyocell stabilizers instead of PG: the color formation in Lyocell spinning dopes seemed to be much less, which prompted us to study the formation of chromophoric compounds from the gallate derivatives in more detail and to compare the chromophore-generation potential

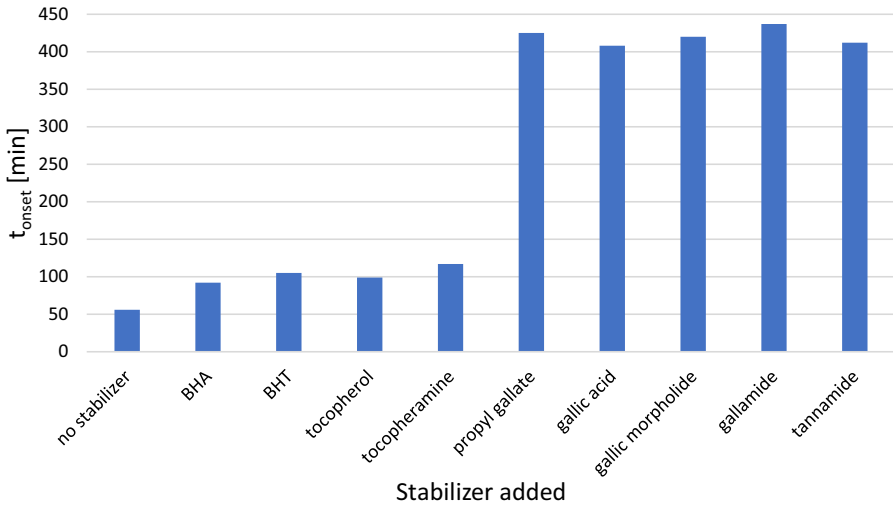

Fig. 4 Times t_{onset} (min) until the start of the uncontrolled exothermic degradation of Lyocell spinning dopes (10 wt% cellulose, 100 °C), induced by 25 ppm Fe(II) sulfate, in dependence of different stabilizers added (0.2 mol% rel. to NMMO monohydrate). Values are averages of three independent measurements (SD < 6% of t_{onset})

of gallic acid (**2**) to its ester (PG, **1**) and amide (**7**–**9**) derivatives, simply by comparison of the UV absorption. The discoloration of the dope was much lower in the case of gallic amides than in the cases of PG or gallic acid.

Figure 5 shows the absorption of the spinning dope at 457 nm—the wavelength for the classical ISO brightness determination—after 30 min, 1 h, 2 h and 4 h at 100 °C in dependence of the stabilizer used (as above, 0.2 mol% rel. to NMMO monohydrate). For better comparison, the values are given relative to the starting value for PG, which was set to unity. It was evident that there were two compound groups whose members each behaved quite similarly: gallic acid and propyl gallate on one side, and the gallic amide derivatives on the other side, with the latter group generating much less color. The difference became especially obvious at longer reaction times (2 h and 4 h in Fig. 5). After 4 h, the absorption of the dope stabilized with PG was about five times stronger than in the case of the amide derivatives, and even seven times in the case of gallic acid vs. the respective amides. In general, the absorption/discoloration in the case of the amide derivatives was only approx. 15–25% of gallic esters or gallic acid. Differences between the three amide samples were insignificant.

Also a tannin sample was used as a stabilizer because gallotannins contain high amounts of gallic ester moieties as central structural elements, esterified with themselves (depsides) and with carbohydrates, mostly D-glucopyranose. Interestingly, the color generation turned significantly lower when these

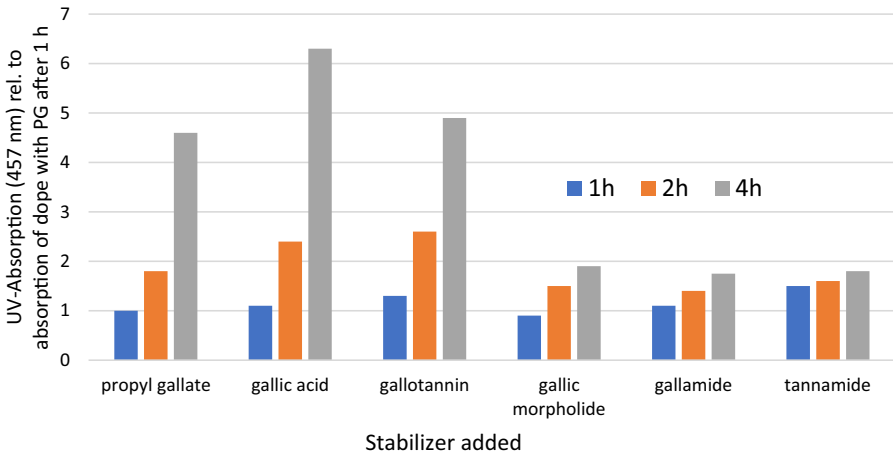

Fig. 5 Color formation in Lyocell spinning dopes (10 wt% pulp rel. to NMMO monohydrate, 100 °C) after different times (1 h, 2 h, 4 h) in dependence of the stabilizer used (0.2 mol% rel. to NMMO monohydrate), measured as UV-absorption at 457 nm. Values are averages of three independent measurements and are given relative to the starting value for PG (set to unity)

esters were converted beforehand to amides by direct aminolysis and the crude tannamide products were used as stabilizers. The behavior of the gallotannins was thus completely analogous to the PG case. This observation of less chromophore generation from the amide derivatives of gallic acid might offer interesting perspectives for the development of bio-based Lyocell stabilizers, and as well a niche valorization of tannins. This will be the subject of a separate report in due course.

The reason for the stronger chromophore generation of gallic acid and PG compared to the more innocuous amide derivatives lies in the ability of the compounds to form ellagic acid and—by further oxidation—the strongly chromophoric ellagoquinone. The formation of ellagic acid from the amide derivatives was only approx. 5–8% of that from gallic acid or propyl gallate. The low reactivity of the gallamides, i.e., their inability to form ellagic acid and the ellagoquinone, eventually translates into a lower chromophore load and less demanding fiber bleaching.

Immediate precursors for ellagic acid formation are the corresponding OH-substituted diphenic acid (**5** in Scheme 1), diphenic acid dipropyl ester (**6**, see Scheme 1) and diphenic acid diamide. They are formed from gallic acid (**2**), PG (**1**) and gallamide (**8**), respectively, by dehydrogenative dimerization, i.e., the coupling of the respective phenoxyl radicals, a key process in the antioxidant action of these compounds. The formation of ellagic acid would be an esterification for diphenic acid (**5**), a transesterification for diphenic acid dipropyl ester (**6**) and an amide-to-ester conversion for the diphenic acid diamide. In all three cases, the reaction forms a lactone structure, i.e. there is an important entropic contribution, providing a significant contribution to the thermodynamic driving force: the release of two small molecules (water, *n*-propanol, or ammonia, respectively) per equivalent of ellagic acid formed. This results in a strongly positive free reaction entropy, which renders the free Gibbs energy more negative (*cf.* the Gibbs equation $\Delta_R G = \Delta_R H - T^* \Delta_R S$), see Table 4. The difference in the formation of ellagic acid must thus be a kinetic factor, rather than a thermodynamic one: the main difference lies in the reactivity of the carboxylic functionalities. While the carboxylic acid and the ester are readily susceptible to nucleophilic attack by the adjacent phenolic hydroxy groups and thus easily undergo (trans)esterification under ring closure, the amide functionalities have a different reactivity: the C–N bond has partial double bond character, the amide group is resonance-stabilized and less prone to nucleophilic substitution, corresponding to

Table 4 Formation of ellagic acid from the diacid, diester and diamide precursors. Computational results

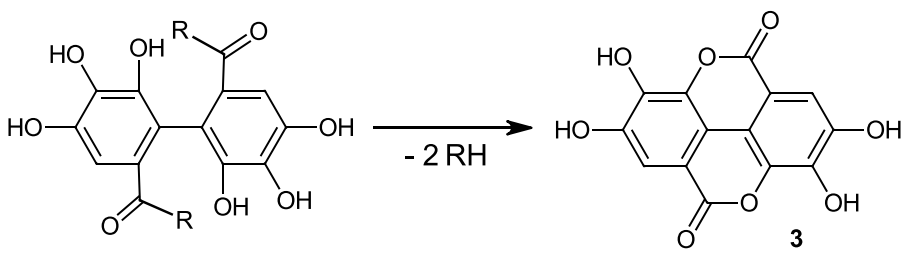

R	ΔE^a	ΔG^{oa}	Atomic charge[b]	Bond order[b]	
			Carbon in C=O	C=O	OC–R
OH	+8.3	−10.4	+0.831	1.73	1.04
OCH_3	+18.7	−3.9	+0.842	1.72	1.03
NH_2	+13.2	−5.4	+0.690	1.66	1.20

[a]Energies in kcal/mol. Gibbs energies (gas phase) were calculated at 298.15 K and 1 atm. DFT(M06-2X) with basis functions of 6–311 + G(*d*) for C, O, N, 6-311G(*d*, *p*) for acidic H (OH and NH), and 6-311G for the other H

[b]Results of the NBO analysis for the reactants

general reactivity rules that prohibit direct ester formation from amides by alcoholysis, while the opposite process—amides from esters by aminolysis—is generally allowed (Becker 2001). This leads to a high activation energy barrier in the amide case and pronounced kinetic hindrance. The reaction behavior of the gallic derivatives was corroborated by computations, carried out at the DFT(M06-2X) level of theory (Table 4).

Conclusions

Propyl gallate, long used as an antioxidant in food science and general polymer science, had also been established as a stabilizer for cellulose solutions in *N*-methylmorpholine-*N*-oxide for the reasons of good efficiency, availability and economic viability. However, under real-world conditions, mainly by the action of the alkaline byproducts morpholine and *N*-methylmorpholine derived from NMMO, it is rapidly converted into gallate by hydrolysis. Aminolysis to gallic morpholide is an additional, secondary side process. This raises the questions of whether propyl gallate itself has to be used or whether this use is rather a "detour" and the hydrolysis products can be used directly—this would of course only be possible if they show a similarly good stabilizing effect.

As our study shows, gallic acid, gallic morpholide—as well as other gallamides used for comparison—indeed had the same stabilizing effect on lyocell dopes as PG itself. Interestingly, however, color generation was significantly lower with gallamides than with PG and gallic acid which—at least potentially—represents a clear advantage. PG and gallic acid form ellagic acid and its dark-colored ellago-quinone as very potent chromophores—this formation pathway is unavailable in gallamides due to the stability of the amide bond.

The finding that gallic acid amide-based stabilizers generate much less color than PG or gallic acid may have interesting practical and also economic implications for the Lyocell process. Fewer chromophores translates into brighter fibers and less oxidative damage to the cellulose since, after all, fewer bleaching chemicals are needed. At the same time, avoiding the formation of ellagic acid species should have a very positive impact on solvent recycling, since the requirements for purification by adsorptive chromophore removal will be much lower.

Future research will now address synthesis aspects of gallamide stabilizers, the structure of the gallotannins from which such compounds can be prepared, and the effect of these auxiliaries on the properties of the manufactured cellulosic fibers, particularly with respect to brightness properties (chromophore formation) and cellulose integrity (oxidative damage). The results of these studies will be reported in due course.

Acknowledgments The authors would like to thank the Austrian Biorefinery Center Tulln (ABCT) for financial support.

Author contributions IM, AP and TRo contributed to the study conception and design. TH contributed to computational chemistry, MB to NMR investigations. Material preparation, data collection and analysis were performed by all authors. The first draft of the manuscript was written by HH and TR and all authors commented on previous versions of the manuscript. All authors read and approved the final manuscript.

Funding Open access funding provided by University of Natural Resources and Life Sciences, Vienna (BOKU). The financial support by the Austrian Biorefinery Center Tulln (ABCT) is gratefully acknowledged.

Data availability Data available from the authors upon request.

Code availability Not applicable.

Declarations

Conflict of interest None.

Ethical approval Not applicable.

Consent to participate Not applicable.

Consent for publication All authors agreed to the publication in the submitted form.

References

Adegoke GO, Vijay Kumar M, Gopala Krishna AG, Varadaraj MC, Sambaiah K, Lokesh BR (1989) Antioxidants and lipid oxidation in foods - a critical appraisal. J Food Sci Technol 35(4):283–298

Ahn K, Zaccaron S, Zwirchmayr NS, Hettegger H, Hofinger H, Bacher M, Henniges U, Hosoya T, Potthast A, Rosenau T (2019) Yellowing and brightness reversion of celluloses: CO or COOH, who is the culprit? Cellulose 26:429–444

Akanbi TO, Barrow CJ (2018) Enzymatic production of antioxidants and their applications. In: Varelis P, Melton L, Shahidi F (eds) Encyclopedia of food chemistry. Elsevier, Amsterdam, pp 92–96

Albini A (1993) Synthetic utility of amine N-oxides. Synthesis 1993:263–277

Amadasi A, Mozzarelli A, Meda C, Maggi A, Cozzini P (2009) Identification of xenoestrogens in food additives by an integrated in silico and in vitro approach. Chem Res Toxicol 22(1):52–63

Anderson KE, Conney AH, Kappas A (1982) Effects of dietary fat, butylated hydroxytoluene and propyl gallate on microsomal drug metabolism in rats. Nutrition Rev 40(6):189–191

Aslanzadeh S, Berg A, Taherzadeh MJ, Sárvári Horváth I (2014) Biogas production from N-Methylmorpholine-N-oxide (NMMO) pretreated forest residues. Appl Biochem Biotechnol 172(6):2998–3008

Becker HGO (2001) Organikum, 21st edn. Wiley-VCH, Weinheim

Becker I (2007) Final report on the amended safety assessment of propyl gallate. Int J Toxicol 26(suppl. 3):89–118

Böhmdorfer S, Oberlerchner JS, Fuchs C, Rosenau T, Grausgruber H (2018) Profiling and quantification of grain anthocyanins in purple pericarp × blue aleurone wheat crosses by high-performance thin-layer chromatography and densitometry. Plant Methods 14(29):2–15

Cai LY, Ma YL, Ma XX, Lv JM (2016) Improvement of enzymatic hydrolysis and ethanol production from corn stalk by alkali and N-methylmorpholine-N-oxide pretreatments. Biores Technol 212:42–46

Chỳlková J, Tomášková M, Jehlička V, Švancara I, Šelešovská R (2017) The electrochemical determination of the synthetic antioxidants used as stabilizers in mineral oils and biofuel. Adv Chem Res 37:1–13

Coleman KS, Bedel LJL, Osborn JA (2000) Catalytic oxidation of alcohols to aldehydes or ketones using osmium-oxo complexes with sulfoxides or N-methylmorpholine-N-oxide as the co-oxidant: a comparative study. Comptes Rendus Acad Sci - Ser IIc: Chemistry 3(10):765–769

Decker EA, Chen B, Panya A, Elias RJ (2010) Understanding antioxidant mechanisms in preventing oxidation in foods. Oxidation in foods and beverages and antioxidant applications. Elsevier Inc., Amsterdam, pp 225–248

Dolatabadi JEN, Kashanian S (2010) A review on DNA interaction with synthetic phenolic food additives. Food Res Int 43(5):1223–1230

Erdman A, Kulpinski P, Grzyb T, Lis S (2016) Preparation of multicolor luminescent cellulose fibers containing lanthanide doped inorganic nanomaterials. J Luminescence 169:520–527

Fink HP, Weigel P, Purz HJ, Ganster J (2001) Structure formation of regenerated cellulose materials from NMMO-solutions. Progr Polym Sci 26(9):1473–1524

Firgo H, Eibl M, Eichinger D (1995) Lyocell - an ecological alternative. Lenzinger Ber 75:47–50

Gamboni SE, Palmer AM, Nixon RL (2013) Allergic contact stomatitis to dodecyl gallate? A review of the relevance of positive patch test results to gallates. Australasian J Dermatol 54(3):213–217

Gómez-Hens A, Godoy-Navajas J (2015) Determination of propyl, octyl, and dodecyl gallates. In: Ruiz-Capillas C, Nollet LML (eds) Flow injection analysis of food additives, 1st edn. CRC Press, Oxford, pp 241–260

Goshadrou A, Karimi K, Taherzadeh MJ (2013) Ethanol and biogas production from birch by NMMO-pretreatment. Biomass Bioenergy 49:95–101

Gregor W, Grabner G, Adelwöhrer C, Rosenau T, Gille L (2005) Antioxidant properties of natural and synthetic chromanol derivatives: a study by fast kinetics and electron spin resonance spectroscopy. J Org Chem 70(9):3472–3483

Hirose M, Yada H, Hakoi K, Takahashi S, Ito N (1993) Modification of carcinogenesis by α-tocopherol, t-butylhydroquinone, propyl gallate and butylated hydroxytoluene in a rat multi-organ carcinogenesis model. Carcinogenesis 14(11):2359–2364

Holcomb ZE, van Noord MG, Atwater AR (2017) Gallate contact dermatitis: product update and systematic review. Dermatitis 28(2):115–127

Jusner P, Bacher M, Simon J, Bausch F, Khaliliyan H, Schiehser S, Sumerskii I, Schwaiger E, Potthast A, Rosenau T (2022) Analyzing the effects of thermal stress on insulator papers by solid-state ^{13}C NMR spectroscopy. Cellulose 29(2):1081–1095

Kahl R (1984) Synthetic antioxidants: Biochemical actions and interference with radiation, toxic compounds, chemical mutagens and chemical carcinogens. Toxicology 33(3–4):185–228

Kawanishi S, Oikawa S, Murata M (2005) Evaluation for safety of antioxidant chemopreventive agents. Antiox Redox Signal 7(11–12):1728–1739

Khodaverdi M, Jeihanipour A, Karimi K, Taherzadeh MJ (2012) Kinetic modeling of rapid enzymatic hydrolysis of crystalline cellulose after pretreatment by NMMO. J Ind Microbiol Biotechnol 39:429–438

Kobayashi H, Murata M, Kawanishi S, Oikawa S (2020) Polyphenols with anti-amyloid β aggregation show potential risk of toxicity via pro-oxidant properties. Int J Mol Sci 21(10):3561

Komaitis ME (1991) Thin layer chromatographic detection of some common antioxidants. Grasas Aceites 42(6):420–421

Korntner P, Hosoya T, Dietz T, Eibinger K, Reiter H, Spitzbart M, Röder T, Borgards A, Kreiner W, Mahler AK, Winter H, French AD, Henniges U, Potthast A, Rosenau T (2015) Chromophores in lignin-free cellulosic materials belong to three compound classes. Cellulose 22(2):1053–1062

Kulpinski P, Namyslak M, Grzyb T, Lis S (2012) Luminescent cellulose fibers activated by Eu 3+-doped nanoparticles. Cellulose 19(4):1271–1278

Kumar V, Sai GM, Verma R, Mitchell-Koch KR, Ray D, Aswal VK, Thareja P, Kuperkar K, Bahadur P (2021) Tuning cationic micelle properties with an antioxidant additive: a molecular perspective. Langmuir 37(15):4611–4621

Kuo CH, Lee CK (2009) Enhanced enzymatic hydrolysis of sugarcane bagasse by N-methylmorpholine-N-oxide pretreatment. Biores Technol 100:866–871

Liu Y, Zhong Q, Wang S, Cai Z (2011) Correlating physical changes and enhanced enzymatic saccharification of pine flour pretreated by N-methylmorpholine-N-oxide. Biomacromol 12(7):2626–2632

Marini I, Brauneis F (1996) Lyocell - die wichtigsten unterschiede zu den anderen cellulosischen Fasern. Textilveredlung 31:182–187

Morton DR, Thompson JL (1978) Total synthesis of 3-oxa-4,5,6-trinor-3,7-inter-m-phenylene prostaglandins. 2. Conjugate addition approach. J Org Chem 43(11):2102–2106

Oberlerchner JT, Böhmdorfer S, Rosenau T, Potthast A (2018) A matrix-resistant HPTLC method to quantify monosaccharides in wood-based lignocellulose biorefinery streams. Holzforschung 72(8):645–652

Oswell NJ, Thippareddi H, Pegg RB (2018) Practical use of natural antioxidants in meat products in the U.S.: a review. Meat Sci 145:469–479

Ow YY, Stupans I (2003) Gallic acid and gallic acid derivatives: effects on drug metabolizing enzymes. Curr Drug Metabol 4(3):241–248

Öztürk HB, Potthast A, Rosenau T, Abu-Rous M, MacNaughtan B, Schuster KC, Mitchell J, Bechtold T (2009) Changes in the intra- and interfibrillar structure of lyocell (Tencel®) fibers caused by NaOH treatment. Cellulose 16(1):37–52

Poornejad N, Karimi K, Behzad T (2013) Improvement of saccharification and ethanol production from rice straw by NMMO and [BMIM][OAc] pretreatments. Ind Crops Prod 41:408–413

Potthast A, Rosenau T, Henniges U, Schiehser S, Kosma P, Saake B, Lebioda S, Radosta S, Vorwerg W, Wetzel H, Koschella A, Heinze T, Strobin G, Sixta H, Strlic M, Isogai A (2015) Comparison testing of methods for gel permeation chromatography of cellulose: coming closer to a standard protocol. Cellulose 22(3):1591–613

Rosenau T, Potthast A, Kosma P, Chen CL, Gratzl JS (1999) Autocatalytic decomposition of N-Methylmorpholine-N-oxide induced by mannich intermediates. J Org Chem 64:2166–2167

Rosenau T, Potthast A, Adorjan I, Hofinger A, Sixta H, Firgo H, Kosma P (2002) Cellulose solutions in N-methylmorpholine-N-oxide (NMMO) – degradation processes and stabilizers. Cellulose 9(3–4):283–291

Rosenau T, Hofinger A, Potthast A, Kosma P (2004) A general, selective high-yield N-demethylation procedure for tertiary amines by solid reagents in a convenient column chromatography-like setup. Org Lett 6(4):541–544

Rosenau T, Potthast A, Milacher W, Adorjan I, Hofinger A, Kosma P (2005) Discoloration of cellulose solutions in N-methyl-morpholine-N-oxide (Lyocell). Part 2: Isolation and identification of chromophores. Cellulose 12(2):197–208

Rosenau T, Ebner G, Stanger A, Perl S, Nuri L (2005b) From a theoretical concept to biochemical reactions: strain induced bond localization (SIBL) in oxidation of vitamin E. Chem Eur J 11(1):280–287

Shafiei M, Karimi K, Taherzadeh MJ (2010) Pretreatment of spruce and oak by N-methylmorpholine-N-oxide (NMMO) for efficient conversion of their cellulose to ethanol. Biores Technol 101(13):4914–4918

Shalini M, Kalaivani T, Rajasekaran C (2014) Therapeutic potential of gallic acid and its derivatives: a review. In: Science N (ed) Recent advance in gallate research, kinsey A f. Publishers Inc., Hauppauge, pp 201–227

Shameer MP, Nishath MP (2019) Exploration and enhancement on fuel stability of biodiesel: a step forward in the track of global commercialization. In: Azad AK, Rasul M (eds) Advanced biofuels: applications, technologies and environmental sustainability. Woodhead Publishing, Sawston, pp 181–213

Skwierczyńska M, Runowski M, Kulpiński P, Lis S (2019) Modification of cellulose fibers with inorganic luminescent nanoparticles based on lanthanide(III) ions. Carbohydr Polym 206:742–748

Smiechowicz E, Niekraszewicz B, Kulpinski P, Dzitko K (2018) Antibacterial composite cellulose fibers modified with silver nanoparticles and nanosilica. Cellulose 25(6):3499–3517

Syed Jaafar SN, Baron J, Siebenhandl-Ehn S, Rosenau T, Böhmdorfer S, Grausgruber H (2013) Increased anthocyanin content in purple pericarp × blue aleurone wheat crosses. Plant Breed 132(6):546–552

Taherzadeh MJ, Karimi K (2008) Pretreatment of lignocellulosic wastes to improve ethanol and biogas production: a review. Int J Mol Sci 9(9):1621–1651

Tan YJ, Ali A, Tee SY, Teo JT, Xi Y, Go ML, Lam Y (2019) Galloyl esters of trans-stilbenes are inhibitors of FASN with anticancer activity on non-small cell lung cancer cells. Eur J Med Chem 182:111597

Teghammar A, Karimi K, Horváth IS, Taherzadeh MJ (2012) Enhanced biogas production from rice straw, triticale straw and softwood spruce by NMMO pretreatment. Biomass Bioenergy 36:116–120

Thysiadis S, Katsamakas S, Mpousis S, Avramidis N, Sarli ESV (2018) Design and synthesis of gallocyanine inhibitors of DKK1/LRP6 interactions for treatment of Alzheimer's disease. Bioorg Chem 80:230–244

Walton K, Walker R, van De Sandt JJM, Castell JV, Knapp AGAA, Kozianowski G, Roberfroid M, Schilter B (1999) The application of in vitro data in the derivation of the acceptable daily intake of food additives. Food Chem Toxicol 37(12):1175–1197

Wang W, Xiong P, Zhang H, Zhu Q, Liao C, Jiang G (2021) Analysis, occurrence, toxicity and environmental health risks of synthetic phenolic antioxidants: a review. Environ Res 201:111531

Wikandari R, Millati R, Taherzadeh MJ (2016) Pretreatment of lignocelluloses with solvent N-Methylmorpholine N-oxide. In: Mussatto SI (ed) Biomass fractionation technologies for a lignocellulosic feedstock based biorefinery. Elsevier, Amsterdam, pp 255–280

Yiin CL, Yusup S, Udomsap P, Yoosuk B, Sukkasi S (2014) Stabilization of empty fruit bunch (EFB) derived Bio-oil using antioxidants. Comput Aided Chem Engin 33:223–228

Yokota S, Kitaoka T, Opietnik M, Rosenau T, Wariishi H (2008) Synthesis of gold nanoparticles for in situ conjugation with structural carbohydrates. Angew Chem Int Ed Engl 47:9866–9869

Zhang HY, Yang DP, Tang GY (2006) Multipotent antioxidants: from screening to design. Drug Discov Today 11(15–16):749–754

Zhang S, Chen C, Duan C, Hu H, Li H, Li J, Liu Y, Ma X, Stavik J, Ni Y (2018) Regenerated cellulose by the lyocell process, a brief review of the process and properties. BioRes 13(2):1–16

Zuckerstätter G, Terinte N, Sixta H, Schuster KC (2013) Novel insight into cellulose supramolecular structure through ^{13}C CP-MAS NMR spectroscopy and paramagnetic relaxation enhancement. Carbohydr Polym 93:122–128